

Two-Dimensional Infrared Spectroscopy Reveals Cosolvent-Composition-Dependent Crossover in Intermolecular Hydrogen-Bond Dynamics

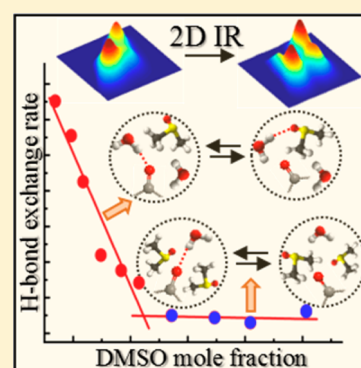
Somnath M. Kashid,[§] Geun Young Jin,[†] Suman Chakrabarty,^{*,§} Yung Sam Kim,^{*,†} and Sayan Bagchi^{*,§}

[§]Physical and Materials Chemistry Division, CSIR-National Chemical Laboratory, Dr. Homi Bhabha Road, Pune 411008, India

[†]Department of Chemistry, Ulsan National Institute of Science and Technology (UNIST), 50 UNIST-gil, Ulsan 44919, Korea

Supporting Information

ABSTRACT: Cosolvents have versatile composition-dependent applications in chemistry and biology. The simultaneous presence of hydrophobic and hydrophilic groups in dimethyl sulfoxide (DMSO), an industrially important amphiphilic cosolvent, when combined with the unique properties of water, plays key roles in the diverse fields of pharmacology, cryoprotection, and cell biology. Moreover, molecules dissolved in aqueous DMSO exhibit an anomalous concentration-dependent nonmonotonic behavior in stability and activity near a critical DMSO mole fraction of 0.15. An experimental identification of the origin of this anomaly can lead to newer chemical and biological applications. We report a direct spectroscopic observation of the anomalous behavior using ultrafast two-dimensional infrared spectroscopy experiments. Our results demonstrate the cosolvent-concentration-dependent nonmonotonicity arises from nonidentical mechanisms in ultrafast hydrogen-bond-exchange dynamics of water above and below the critical cosolvent concentration. Comparison of experimental and theoretical results provides a molecular-level mechanistic understanding: a distinct difference in the stabilization of the solute through dynamic solute–solvent interactions is the key to the anomalous behavior.



Cosolvents, because of their highly sensitive composition-dependent properties, play crucial roles in molecular stability, activity, and self-assembly. Addition of cosolvents not only alters the bulk properties, such as dielectric constant, but also affects local specific interactions, such as hydrogen bonds (H bonds) in the vicinity of the solute molecules. The solute–solvent interactions as well as the solute hydration dynamics show intrinsic dependence on the cosolvent's concentration and composition. The choice of cosolvent has profound effects in the diverse fields of chemistry, biology, and pharmacology—from solubilizing and transporting small organic molecules to disrupting protein conformational equilibrium. Controlling these processes is of both fundamental and technological importance and requires a detailed understanding of the underlying cosolvent-concentration-dependent molecular mechanisms.

Small amphiphilic molecules, when combined with water, exhibit composition-dependent properties as solvent and reaction medium.¹ The simultaneous presence of hydrophobic and hydrophilic groups in these cosolvents, along with the unique properties of water, allows a wide range of molecular functions. The aqueous binary solutions in the right proportion can play key roles in drug delivery and enzymatic activity. Among these binary mixtures, dimethyl sulfoxide (DMSO)–water is industrially relevant and has wide applications in cryoprotection, membrane penetration and transport, anti-

inflammation, cholinesterase inhibition, and nerve blockade.² The versatility of DMSO–water becomes amplified by a concentration-dependent anomalous behavioral crossover of the solute near DMSO mole fraction (χ_{DMSO}) of 0.15.^{3–6} Below the critical mole fraction of 0.15, DMSO–water mixtures act as protein stabilizers and activators; beyond this concentration, they behave as denaturants and inhibitors. Several theoretical and experimental studies investigated the molecular structures and interactions in aqueous DMSO solutions to understand the behavioral crossover.^{7–11} Concentration-dependent molecular organizations⁹ as well as a cooperative aggregation phenomenon⁴ have been suggested to be crucial toward the anomalous crossover. The experimental reports on DMSO–water mixtures provide an indirect approach to interrogate the anomaly because they fail to incorporate the solute's response to varying DMSO concentration. A direct experimental identification of the solute's behavioral crossover that can underpin the molecular origin of the anomaly has been missing to date. The cosolvent-concentration-dependent anomalous behavior, unraveled from the solute's perspective, can lead to newer applications of the cosolvent. Understanding the molecular interactions and dynamics, the two major contributors to

Received: February 3, 2017

Accepted: March 22, 2017

Published: March 22, 2017

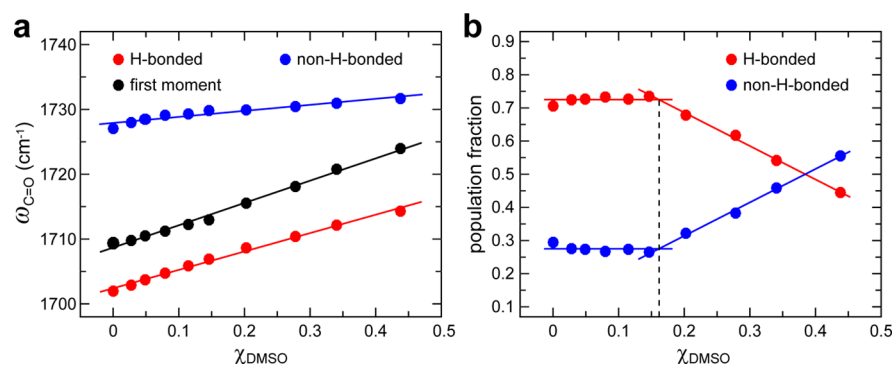


Figure 1. (a) Monotonic change in the first moments of C=O stretch absorption spectra (black), deconvoluted H-bonded (red), and non-H-bonded (blue) C=O peak frequencies with change in χ_{DMSO} . (b) Nonmonotonic change in H-bonded (red) and non-H-bonded (blue) C=O population fraction as a function of χ_{DMSO} . The straight lines represent linear fits to the corresponding data points.

Table 1. Population Mole Fractions and Exchange Rates in Different DMSO–Water Binary Mixtures

solvent (ratio is by volume)	D ₂ O	9 D ₂ O/ 1 DMSO	5 D ₂ O/ 1 DMSO	3 D ₂ O/ 1 DMSO	2 D ₂ O/ 1 DMSO	1.5 D ₂ O/ 1 DMSO	1 D ₂ O/ 1 DMSO	1 D ₂ O/ 1.5 DMSO	1 D ₂ O/ 2 DMSO	1 D ₂ O/ 3 DMSO
H-bonded population mole fraction	0.70	0.72	0.73	0.73	0.73	0.73	0.68	0.62	0.54	0.44
non-H-bonded population mole fraction	0.30	0.28	0.27	0.27	0.27	0.27	0.32	0.38	0.46	0.56
exchange rate (10^{11} s^{-1})	7.50	6.53	5.24	3.18	2.75	2.40	1.48	1.42	1.28	1.69

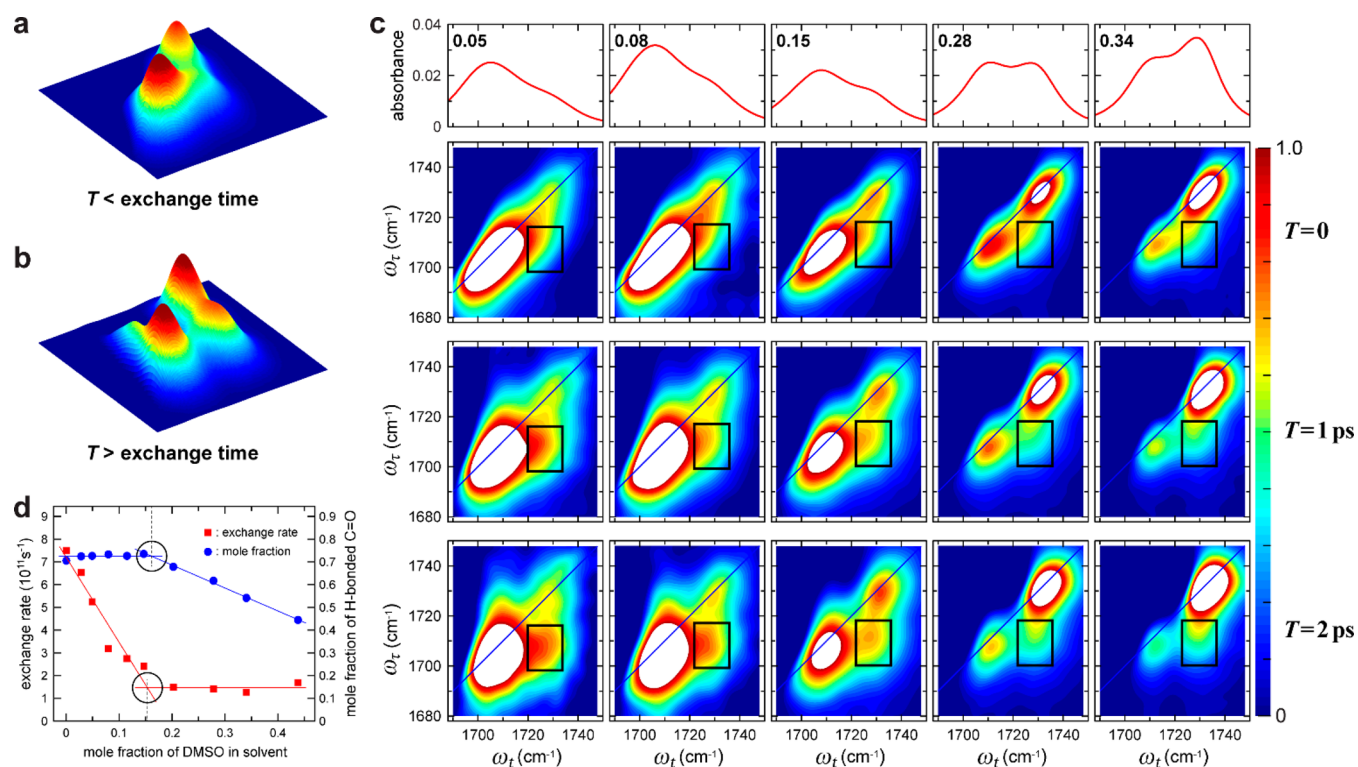


Figure 2. Representative 2D IR spectra showing the presence of (a) diagonal peaks at a waiting time (T) less than the H-bond exchange time scale and (b) diagonal and cross peaks at a waiting time (T) greater than the H-bond exchange time scale. The evolution of T -dependent cross peak is the direct experimental signature of the H-bond making and breaking process. (c) Linear and 2D IR spectra at different waiting times of C=O stretch in DMSO/D₂O mixtures with varying DMSO mole fractions. Only $\nu = 0 \rightarrow 1$ transitions are shown in the 2D IR spectra. Spectral regions for $\nu = 1 \rightarrow 2$ transitions (blue) are not plotted. To compare the magnitude of the cross peaks to the diagonal peaks, the magnitude of each 2D spectrum was referenced to the geometric mean of the two diagonal peaks. Contours of the spectral regions more intense than the geometric mean are not plotted (white). The black rectangle in each 2D spectrum indicates the spectral region of the cross peak arising from the exchange process. (d) C=O H-bond-exchange rate plotted against χ_{DMSO} . The plot of deconvoluted H-bonded C=O population as a function of χ_{DMSO} has been reproduced from Figure 1b to emphasize the nonmonotonic behavior at a similar DMSO concentration of the binary mixture.

structure–function relation, can provide new insights regarding the anomalous concentration dependence of the cosolvent.

The average electric field exerted on the solute by the surrounding solvent molecules provides a quantitative and

microscopic description of the solute–solvent interaction.¹² Vibrational frequencies of carbonyls (C=O), both H-bonded and non-H-bonded, are experimental proxies to electric field through vibrational linear Stark effect.^{12–14} We have performed a series of infrared (IR) absorption experiments on a C=O containing solute (ethyl acetate, EtOAc) in DMSO–water mixtures by varying the mole fraction of the cosolvent in a systematic manner from 0.0 to ~0.5. The absorption spectra of C=O stretch shows two populations. Deconvolution of the experimental spectra using multicomponent fitting shows two bands arising from H-bonded and non-H-bonded C=O. The peak maxima of both the populations shift to higher frequencies with increase in χ_{DMSO} . The first moments of the C=O absorption frequencies, which correspond to the ensemble average electric field along the carbonyl bond (see Table S1 for details),^{15,16} when plotted against DMSO mole fractions, show a linear correlation over the entire DMSO concentration range encompassing the critical mole fraction of 0.15 (Figure 1a). The linear trend in average C=O frequencies indicates a monotonic change in the solute–solvent interactions in terms of electric fields exerted on the solute by the different binary solvent mixtures. Moreover, the linearity of the individual deconvoluted peak maxima of the H-bonded and the non-H-bonded C=O populations with χ_{DMSO} indicates absence of any preferential solvation of the solute within the examined concentration range of DMSO (Figure 1a). These results illustrate that a time-averaged change in the molecular interactions, i.e., concentration-dependent molecular organization of DMSO–water, cannot explain the nonmonotonic behavior in the solute’s properties. The H-bonded and non-H-bonded solute populations obtained from the deconvoluted C=O absorption spectra (peak areas) in different DMSO–water mixtures (Table 1), however, demonstrate an interesting nonmonotonic variation with χ_{DMSO} (Figure 1b). The H-bonded (non-H-bonded) solute population remains unchanged at lower concentrations of DMSO and shows a monotonic decrease (increase) at higher concentrations. A change in either the H-bonded or the non-H-bonded population can be observed at $\chi_{\text{DMSO}} \sim 0.17$, similar to the reported critical mole fraction.

The aforementioned time-averaged results cannot account for the intrinsic solvent dynamics that cause constant making and breaking of H bonds between solute molecules and water in ultrafast (picosecond) time scales. Time-resolved experiments, on the other hand, can provide a deeper insight regarding any role of ultrafast H-bond dynamics in the nonmonotonic anomalous crossover observed for DMSO–water mixtures. Previous studies reported C=O H-bond dynamics in DMSO/water ($\chi_{\text{DMSO}} = 0.2$) to be slower than that in neat water.¹⁷ We have performed two-dimensional infrared (2D IR) spectroscopic experiments to estimate the cosolvent-composition-dependent perturbation in intermolecular H-bond-exchange dynamics between C=O and water. Details about the experimental scheme of chemical exchange 2D IR spectroscopy can be found in earlier published reports.^{11,17–29} In short, 2D IR utilizes three interactions of ultrashort femtosecond pulses at different time delays to generate a nonlinear signal (photon echo) from the sample solution. The first laser pulse simultaneously labels the H-bonded and non-H-bonded C=O groups with their initial frequencies, ω_r . For waiting times (T , time delay between the second and the third pulses) smaller than the H-bond-exchange time scale, most of the labeled species maintain their initial

structures and their final C=O frequencies, ω_b , remain the same as the initial frequencies. A corresponding 2D IR spectrum shows two peaks along the diagonal, which indicates the presence of both H-bonded and non-H-bonded C=O populations (Figure 2a). This is consistent with the bimodal distribution in the IR absorption spectrum. Because of inherent solvent fluctuations leading to H-bond making and breaking, the interconversion between the H-bonded and the non-H-bonded populations is manifested in the 2D IR spectrum by the evolution of T -dependent cross peaks (Figure 2b) for time delays greater than the H-bond-exchange time scale. 2D IR spectra at different waiting times for different DMSO concentrations encompassing $\chi_{\text{DMSO}} = 0.15$ are shown in Figure 2c. The accurate kinetic rates of the hydrogen-bond exchange (Tables 1 and S2) for each composition of DMSO–water mixture have been obtained from the least-squares fitting of the corresponding numerically simulated 2D IR spectra.¹⁷ Though the ultrafast H-bond exchange process is not apparent from the time-averaged linear absorption spectra, the simulated 2D IR spectra reveal that inclusion of chemical exchange captures most of the experimental 2D IR spectral features, including the T -dependent cross peaks (Figures S1–S9). The chemical-exchange rate shows a monotonic decrease with increase in χ_{DMSO} at low DMSO concentrations. Beyond a certain χ_{DMSO} , however, the H-bond-exchange rate estimated from 2D IR is almost independent of the DMSO concentration (Figure 2d). The binary solvent mixture composition at which the initial monotonic decrease in H-bond-exchange dynamics time scale is arrested corresponds to $\chi_{\text{DMSO}} = 0.15$, very similar to the composition that shows the change in hydrogen-bonded population (Figure 2d). These results demonstrate that a change in solute–solvent hydrogen-bond-exchange dynamics mediates the anomalous crossover at $\chi_{\text{DMSO}} \sim 0.15$. Moreover, the biphasic trend in the concentration dependence of the H-bond dynamics indicates a plausible change in the molecular mechanism of the H-bond making and breaking process. Earlier theoretical reports indicated a possible role of solvent dynamics; however, a quantitative experimental observation had been lacking.⁴

A comparison of the experimental results with those obtained from molecular dynamics (MD) simulations can provide a molecular-level understanding of the role of H-bond dynamics toward the anomalous crossover. H-bond population analysis from the simulation trajectories illustrates that the C=O can form zero, one, or two H bonds with the surrounding water molecules. The change in H-bonded C=O population (including both single and double H bonds) with χ_{DMSO} shows a similar trend (Figure 3a), as seen from IR absorption spectra (Figure 2c). H-bond dynamics between C=O and water have been estimated from simulations in different DMSO–water mixtures using earlier reported protocols (refer to the Supporting Information for simulation details).⁸ Autocorrelation of a binary function, either zero for non-H-bonded or one for H-bonded, provides the H-bond-exchange time scale. The variation of the C=O H-bond-exchange rate with χ_{DMSO} shows a similar biphasic trend as obtained from 2D IR experiments (Figure 3b), indicating the existence of two different dynamic mechanisms above and below the critical mole fraction of DMSO. Unlike the 2D IR results, the exchange rates obtained from simulations are not constant for $\chi_{\text{DMSO}} > 0.15$; however, there is a considerable slowdown in the change of H-bond kinetics. The autocorrelation traces for the DMSO–water mixtures were fitted to a triexponential function (Table

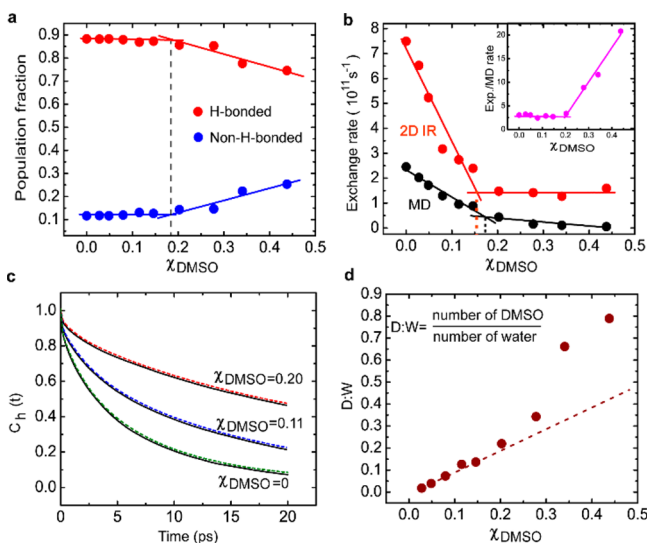


Figure 3. Results from MD simulations. (a) Nonmonotonic change in H-bonded (red) and non-H-bonded (blue) C=O population fraction as a function of χ_{DMSO} . (b) C=O H-bond-exchange rates from 2D IR (red) and MD simulations (black) as a function of χ_{DMSO} . The ratio of experimental and simulated exchange rates, as shown in the inset, are constant around $\chi_{\text{DMSO}} = 0.15$, and changes in the relative rates are observed only at much larger values of χ_{DMSO} . The straight lines represent linear fits to the corresponding data points. (c) Representative autocorrelation traces (dotted) and their respective triexponential fits (solid). (d) Number of DMSO molecules per water molecule in the first solvation shell plotted against χ_{DMSO} .

S3). Figure 3c shows the autocorrelation traces for three representative DMSO–water mixtures along with the triexponential fits. All the fits have a sub-150 fs ultrafast decay component, which is on the time scale predicted for the librational motions of the water molecules.³⁰ A slower time scale of ~ 2.5 ps is observed for all binary mixtures, which quantitatively matches with the H-bond-exchange time scale of bulk water attributed to the reorientational motion of water.³¹ This component involves either exchange between two water molecules already present in the first solvation shell of the probe molecule (Figure 4, top panel) or dynamic breakage and reformation of a hydrogen bond with the same water molecule. The corresponding amplitude, however, decreases with increase in χ_{DMSO} because of emergence of another much slower time scale (>20 ps) process. The time constant and the corresponding amplitude of this component increase dramatically with increasing χ_{DMSO} , which can be attributed to the exchange between water and DMSO in the first solvation shell of C=O (Figure 4, bottom panel). A sudden increase in the number of DMSO molecules per molecule of water within the first solvation shell of the C=O is observed above $\chi_{\text{DMSO}} = 0.15$ (Figure 3d).

A closer look into the MD snapshots reveals two different H-bond-exchange mechanisms (top and bottom panels of Figure 4) for two regimes of DMSO composition. Below $\chi_{\text{DMSO}} = 0.15$, the hydrogen-bond dynamics is dominated by the process of exchange between two different water molecules or same water molecule in the first solvation shell of the solute. This exchange is increasingly hindered by the DMSO molecules that would compete with C=O to form H bonds with water. Subsequent to a C=O–water H-bond breakage, the water molecule may intermittently form a H bond with a DMSO molecule (top panel of Figure 4). Because the DMSO–water H

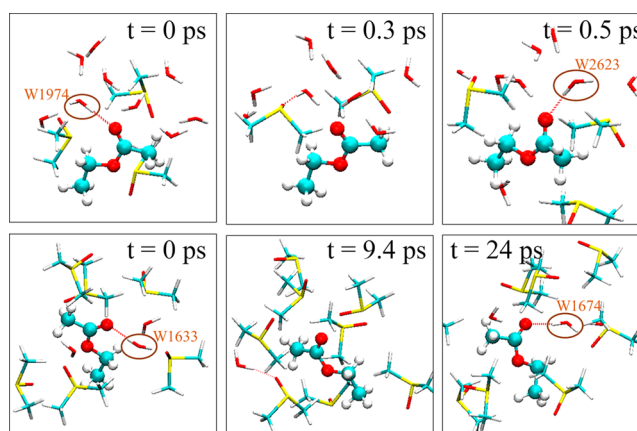


Figure 4. MD snapshots showing the two different H-bond making–breaking mechanisms. The top panel shows competition between DMSO and C=O to form H bonds with water (indirect mechanism). The bottom panel shows direct interaction of DMSO with C=O upon H-bond breaking (direct mechanism). The time scales for the indirect mechanism is much faster than that of the direct mechanism.

bond is stronger compared to water–water or C=O–water H bond, this indirect participation of DMSO in turn slows the C=O–water H-bond-exchange process. This is also manifested in the decrease of double H-bonded C=O and the increase of single H-bonded C=O (Figure S10), while the overall H-bonded C=O population remains constant.

Above the critical mole fraction, the increased density of DMSO in the first solvation shell allows DMSO to directly interact with C=O. Multiple DMSO molecules are positioned near the C=O and occlude the water molecules from reforming H bonds with C=O, once broken. This is also manifested in the H-bond population. Because C=O cannot form a H bond with DMSO, the H-bonded (non-H-bonded) population decreases (increases) for $\chi_{\text{DMSO}} > 0.15$. The slowest time scale obtained from fitting the autocorrelation decay (>20 ps) thereby corresponds to the exchange of water molecules between first solvation shell and bulk, which would become limited by the slow diffusion of DMSO around C=O. A percolation transition due to collective DMSO–water H-bond-network formation had been suggested in an earlier theoretical study.⁴ Thus, beyond a certain DMSO concentration, the diffusion of water molecules becomes limited by the much slower diffusion of the DMSO molecules (Figure S11). This phenomenon, in turn, slows the H-bond-exchange dynamics between C=O and water because water needs to replace the DMSO molecules in the first solvation shell in order to (re)form the H bonds with C=O. Interestingly, experimental results show a constant exchange rate above the critical mole fraction of DMSO (Figure 2d). One of the plausible explanations for the slightly different trends in the exchange rates above $\chi_{\text{DMSO}} = 0.15$ obtained from 2D IR and MD simulations can be due to the slower time scale of DMSO fluctuation dynamics as compared to the experimental time window.

The 2D IR results provide direct experimental proof of the role of solute–solvent H-bond-exchange dynamics toward the crossover anomaly in DMSO–water mixtures. Comparing these results with MD simulations underpins the molecular mechanisms of the H-bond making and breaking process. Our results suggest a distinct difference in the stabilization of the solute molecules through dynamic solute–solvent interactions

happening in ultrafast time scale is the key to the anomalous crossover. An extrapolation of these results to proteins can plausibly explain the switching in protein stability above and below the critical mole fraction of the cosolvent. The indirect interaction of DMSO with the protein below the critical mole fraction does not alter the total number of H bonds of the backbone C=O. A decrease in the overall dielectric constant with addition of a small amount of the cosolvent in turn can make the existing C=O H bonds stronger, leading to an increasing stability of the protein structure. Above the critical mole fraction, the cosolvent directly interacts with the solute C=O resulting in a weakening of the C=O H bonds. Because the H bonds have profound effects on protein stability, a direct interaction thereby leads to instability of the protein structure. The H-bond interactions, however, are transient in nature; thus, the direct experimental observation requires an ultrafast spectroscopic technique capable of detecting the H-bond making and breaking process.

EXPERIMENTAL METHODS

Solutions of 40 mM EtOAc in D₂O and DMSO/D₂O mixture were used for the linear IR absorption and the 2D IR experiments. EtOAc, D₂O, and DMSO were purchased from Sigma-Aldrich and used without further purification. All the reported spectra were collected at room temperature (22 °C). The Fourier-transform infrared (FTIR) absorption spectra were recorded on a Shimadzu IRTracer-100 spectrometer with 0.25 cm⁻¹ resolution. For each sample, ~8 μL of the sample solution was loaded in a demountable sample cell consisting of two CaF₂ windows separated by a Teflon spacer of 25 μm thickness. All 2D IR spectra shown here were collected with parallel polarization and represent the real part of the absorptive (correlation) spectra. The 2D spectra are displayed as the double Fourier transforms of the (τ, t) data set with frequency arguments (ω_ν, ω_t). The details of 2D IR spectroscopy and molecular dynamics simulations are given in the [Supporting Information](#).

ASSOCIATED CONTENT

Supporting Information

The Supporting Information is available free of charge on the ACS Publications website at DOI: [10.1021/acs.jpclett.7b00270](https://doi.org/10.1021/acs.jpclett.7b00270).

Detailed description of the experimental methods and simulation protocols, 2D IR figures, and tables showing fits to experimental and simulation data ([PDF](#))

AUTHOR INFORMATION

Corresponding Authors

*E-mail: s.bagchi@ncl.res.in.

*E-mail: kimys@unist.ac.kr.

*E-mail: s.chakrabarty@ncl.res.in.

ORCID

Suman Chakrabarty: [0000-0002-9461-0015](https://orcid.org/0000-0002-9461-0015)

Sayan Bagchi: [0000-0001-6932-3113](https://orcid.org/0000-0001-6932-3113)

Notes

The authors declare no competing financial interest.

ACKNOWLEDGMENTS

Authors are grateful to Prof. Biman Bagchi for insightful scientific discussion and suggestions. S.B. thanks CSIR-NCL and SERB, India (SR/S2/RJN-142/2012) for financial support.

S.C. thanks SERB, India (SR/S2/RJN-84/2012) and CSIR XIIth five year plan project on Multiscale modelling (CSC0129) for funding. Y.S.K. acknowledges financial support from the National Research Foundation of Korea (Grant 2011-0015061) and the 2010 Research Fund of UNIST, Korea.

REFERENCES

- (1) Zhang, X.; Zhu, Y.; Granick, S. Hydrophobicity at a Janus Interface. *Science* **2002**, *295*, 663–666.
- (2) Jacob, S. W.; Herschler, R. Pharmacology of DMSO. *Cryobiology* **1986**, *23*, 14–27.
- (3) Ghosh, R.; Banerjee, S.; Chakrabarty, S.; Bagchi, B. Anomalous Behavior of Linear Hydrocarbon Chains in Water–DMSO Binary Mixture at Low DMSO Concentration. *J. Phys. Chem. B* **2011**, *115*, 7612–7620.
- (4) Roy, S.; Bagchi, B. Solvation Dynamics of Tryptophan in Water-Dimethyl Sulfoxide Binary Mixture: In Search of Molecular Origin of Composition Dependent Multiple Anomalies. *J. Chem. Phys.* **2013**, *139*, 034308.
- (5) Roy, S.; Banerjee, S.; Biyani, N.; Jana, B.; Bagchi, B. Theoretical and Computational Analysis of Static and Dynamic Anomalies in Water–DMSO Binary Mixture at Low DMSO Concentrations. *J. Phys. Chem. B* **2011**, *115*, 685–692.
- (6) Roy, S.; Jana, B.; Bagchi, B. Dimethyl Sulfoxide Induced Structural Transformations and Non-Monotonic Concentration Dependence of Conformational Fluctuation around Active Site of Lysozyme. *J. Chem. Phys.* **2012**, *136*, 115103.
- (7) Borin, I. A.; Skaf, M. S. Molecular Association between Water and Dimethyl Sulfoxide in Solution: The Librational Dynamics of Water. *Chem. Phys. Lett.* **1998**, *296*, 125–130.
- (8) Luzar, A.; Chandler, D. Structure and Hydrogen-Bond Dynamics of Water-Dimethyl Sulfoxide Mixtures by Computer-Simulations. *J. Chem. Phys.* **1993**, *98*, 8160–8173.
- (9) Soper, A. K.; Luzar, A. A Neutron-Diffraction Study of Dimethyl-Sulfoxide Water Mixtures. *J. Chem. Phys.* **1992**, *97*, 1320–1331.
- (10) Vaisman, II; Berkowitz, M. L. Local Structural Order and Molecular Associations in Water DMSO Mixtures - Molecular-Dynamics Study. *J. Am. Chem. Soc.* **1992**, *114*, 7889–7896.
- (11) Wong, D. B.; Sokolowsky, K. P.; El-Barghouthi, M. I.; Fenn, E. E.; Giammanco, C. H.; Sturlaugson, A. L.; Fayer, M. D. Water Dynamics in Water/DMSO Binary Mixtures. *J. Phys. Chem. B* **2012**, *116*, 5479–5490.
- (12) Fried, S. D.; Boxer, S. G. Measuring Electric Fields and Noncovalent Interactions Using the Vibrational Stark Effect. *Acc. Chem. Res.* **2015**, *48*, 998–1006.
- (13) Fried, S. D.; Bagchi, S.; Boxer, S. G. Measuring Electrostatic Fields in Both Hydrogen-Bonding and Non-Hydrogen-Bonding Environments Using Carbonyl Vibrational Probes. *J. Am. Chem. Soc.* **2013**, *135*, 11181–11192.
- (14) Fried, S. D.; Bagchi, S.; Boxer, S. G. Extreme Electric Fields Power Catalysis in the Active Site of Ketosteroid Isomerase. *Science* **2014**, *346*, 1510–1514.
- (15) Kashid, S. M.; Bagchi, S. Experimental Determination of the Electrostatic Nature of Carbonyl Hydrogen-Bonding Interactions Using IR-NMR Correlations. *J. Phys. Chem. Lett.* **2014**, *5*, 3211–3215.
- (16) Halder, T.; Kashid, S. M.; Deb, P.; Kesh, S.; Bagchi, S. Pick and Choose the Spectroscopic Method to Calibrate the Local Electric Field Inside Proteins. *J. Phys. Chem. Lett.* **2016**, *7*, 2456–2460.
- (17) Kashid, S. M.; Jin, G. Y.; Bagchi, S.; Kim, Y. S. Cosolvent Effects on Solute–Solvent Hydrogen-Bond Dynamics: Ultrafast 2D IR Investigations. *J. Phys. Chem. B* **2015**, *119*, 15334–15343.
- (18) Candelaresi, M.; Pagliai, M.; Lima, M.; Righini, R. Chemical Equilibrium Probed by Two-Dimensional IR Spectroscopy: Hydrogen Bond Dynamics of Methyl Acetate in Water. *J. Phys. Chem. A* **2009**, *113*, 12783–12790.
- (19) Chuntunov, L.; Pazos, I. M.; Ma, J.; Gai, F. Kinetics of Exchange between Zero-, One-, and Two-Hydrogen-Bonded States of Methyl

and Ethyl Acetate in Methanol. *J. Phys. Chem. B* **2015**, *119*, 4512–4520.

(20) Fecko, C. J.; Eaves, J. D.; Loparo, J. J.; Tokmakoff, A.; Geissler, P. L. Ultrafast Hydrogen-Bond Dynamics in the Infrared Spectroscopy of Water. *Science* **2003**, *301*, 1698–1702.

(21) Kim, Y. S.; Hochstrasser, R. M. Chemical Exchange 2D IR of Hydrogen-Bond Making and Breaking. *Proc. Natl. Acad. Sci. U. S. A.* **2005**, *102*, 11185–11190.

(22) Kim, Y. S.; Hochstrasser, R. M. The 2D IR Responses of Amide and Carbonyl Modes in Water Cannot Be Described by Gaussian Frequency Fluctuations. *J. Phys. Chem. B* **2007**, *111*, 9697–9701.

(23) Woutersen, S.; Mu, Y.; Stock, G.; Hamm, P. Hydrogen-Bond Lifetime Measured by Time-Resolved 2D-IR Spectroscopy: N-Methylacetamide in Methanol. *Chem. Phys.* **2001**, *266*, 137–147.

(24) Zheng, J.; Kwak, K.; Asbury, J.; Chen, X.; Piletic, I. R.; Fayer, M. D. Ultrafast Dynamics of Solute-Solvent Complexation Observed at Thermal Equilibrium in Real Time. *Science* **2005**, *309*, 1338–1343.

(25) Dunbar, J. A.; Arthur, E. J.; White, A. M.; Kubarych, K. J. Ultrafast 2D-IR and Simulation Investigations of Preferential Solvation and Cosolvent Exchange Dynamics. *J. Phys. Chem. B* **2015**, *119*, 6271–6279.

(26) Gaffney, K. J.; Ji, M.; Odelius, M.; Park, S.; Sun, Z. H-Bond Switching and Ligand Exchange Dynamics in Aqueous Ionic Solution. *Chem. Phys. Lett.* **2011**, *504*, 1–6.

(27) Kim, Y. S.; Hochstrasser, R. M. Comparison of Linear and 2D IR Spectra in the Presence of Fast Exchange. *J. Phys. Chem. B* **2006**, *110*, 8531–8534.

(28) Hamm, P.; Zanni, M. *Concepts and Methods of 2D Infrared Spectroscopy*; Cambridge University Press: Cambridge, U.K., 2011.

(29) Jin, G. Y.; Kim, Y. S. Phase-Resolved Heterodyne-Detected Transient Grating Enhances the Capabilities of 2D IR Echo Spectroscopy. *J. Phys. Chem. A* **2017**, *121*, 1007–1011.

(30) Laage, D.; Hynes, J. T. A Molecular Jump Mechanism of Water Reorientation. *Science* **2006**, *311*, 832–835.

(31) Fayer, M. D. Dynamics of Water Interacting with Interfaces, Molecules, and Ions. *Acc. Chem. Res.* **2012**, *45*, 3–14.